DNS of a turbulent jet impinging on a heated wall

Thibault Dairay
E. Lamballais, V. Fortuné and L.-E. Brizzi

Institute PPRIME,
Department of Fluid Flow, Heat Transfer and Combustion,
CNRS, Université de Poitiers, ENSMA

24/04/2014

Impinging jet

- A fluid issuing from a nozzle impinging on a solid wall
- Efficient tool to optimize flow/wall heat transfer
- Widely used in industrial applications requiring high transfer rates (cooling, drying...)

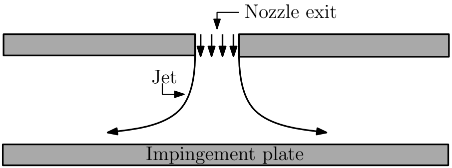

Some applications

Cooling of electronic components

- Increase of computing ressource requirements
- Efficient and simple solution

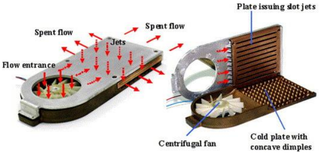

Chang *et al.*, ETFS, 2007

Vertical Take-Off and Landing aircraft

- Vertical force generated by impinging jets
- Control the jets : improve the aircraft stability

Some applications

Cooling of electronic components

- Increase of computing ressource requirements
- Efficient and simple solution

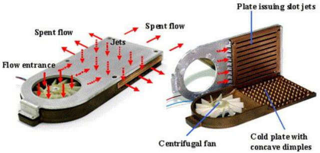

Chang *et al.*, ETFS, 2007

Vertical Take-Off and Landing aircraft

- Vertical force generated by impinging jets
- Control the jets : improve the aircraft stability

Take-off of an AV8B-Harrier ©2013 ForWallpaper.com

Cooling of turbine blades

Industrial challenge

Improve aircraft engine's cooling is a major challenge for the manufacturers

- Optimize the engine efficiency
- Increase its life duration
- Decrease the maintenance cost

Different cooling technics

- Forced internal convection cooling
- Film cooling
- Impinging jet cooling

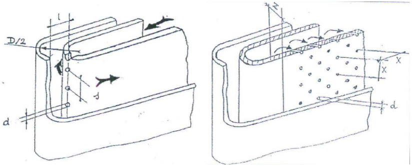

Fénot, PhD Thesis, 2004

At the lab

- Many experimental research at the Institute PPRIME
- Industrial collaboration : DGA, Snecma Moteurs, Turboméca, ONERA

PhD Thesis : Bernard (1997) ; Jolly (2000) ; Brevet (2001) ; Fénot (2004) ; Roux (2011)

Industrial system

Physical analysis : single jet

At the lab

- Many experimental research at the Institute PPRIME
- Industrial collaboration : DGA, Snecma Moteurs, Turboméca, ONERA

PhD Thesis : Bernard (1997) ; Jolly (2000) ; Brevet (2001) ; Fénot (2004) ; Roux (2011)

©SAFRAN
Industrial system

Physical analysis : single jet

At the lab

- Many experimental research at the Institute PPRIME
- Industrial collaboration : DGA, Snecma Moteurs, Turboméca, ONERA

PhD Thesis : Bernard (1997) ; Jolly (2000) ; Brevet (2001) ; Fénot (2004) ; Roux (2011)

©SAFRAN
Industrial system

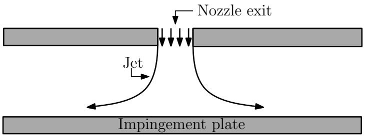

Physical analysis : single jet

Single impinging jet

- A boundary-free shear flow region
- A wall-bounded flow region
- A stagnation region
- Accelerated/decelerated wall jet

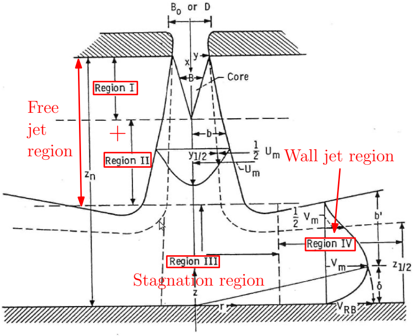

Adapted from

Gauntner *et al.*, TR-NASA, 1970

Single impinging jet : multiple parameters

A lot of possible configurations depending on the choice of geometrical, aerodynamical or thermal parameters :

- Jet type, nozzle-to-plate distance...
- Inflow velocity, Reynolds number...
- Plate heating, temperature difference between the plate, the jet and the surrounding fluid...

Experimental studies

- Review papers of Jambunathan *et al.*, IJHFF, 1992 ; Webb and Ma, AHT, 1995
- PhD thesis of Vejrazka (2002) and Roux (2011)

Numerical studies

- Hadziabdic and Hanjalic, JFM, 2008 ; Dewan *et al.*, HTE, 2012 ; Uddin *et al.*, IJHMT, 2013

Today's motivations

- Secondary maximum in the radial distribution of the mean Nusselt number
- Measurement technics limitations : synchronized temporal evolution of the 3D fields is extremely difficult to obtain, measurement of the near-wall dynamics
- Unsteady numerical studies ($Re \geq 10000$) : exclusively Large Eddy Simulation (LES)

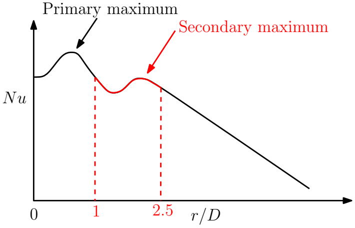

Today's study

DNS of a circular confined jet impinging on a flat plate in a realistic flow regime

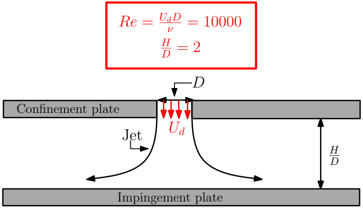

What is the role of unsteady processes to explain the spatial distribution of the mean heat transfer at the wall ?

For experimental validation (PIV, IR Thermography) and comparisons with different LES methodologies, see

Dairay *et al.* under review, IJHFF 2014

Contents

Contents

Problem equations

Incompressible Navier-Stokes equations

$$\begin{aligned} \frac{\partial \mathbf{u}}{\partial t} + \frac{1}{2}\left(\boldsymbol{\nabla} \cdot (\mathbf{u} \otimes \mathbf{u}) + (\mathbf{u} \cdot \boldsymbol{\nabla})\,\mathbf{u}\right) &= -\frac{1}{\rho}\boldsymbol{\nabla} p + \nu \boldsymbol{\nabla}^2 \mathbf{u} \\ \nabla \cdot \mathbf{u} &= 0 \end{aligned}$$

Reynolds number : $Re = \frac{U_d D}{\nu}$

Temperature equation (passive scalar)

$$\frac{\partial T}{\partial t} + \mathbf{u}.\nabla T = \frac{1}{RePr}\nabla^2 T$$

Prandtl number : $Pr = \frac{\nu}{\kappa}$

Incompact3d

Solve the incompressible Navier-Stokes equations on a Cartesian mesh.

- Spatial discretization : High-order compact schemes $O(\Delta x^6)$
- Time advancement : Explicit Adams-Bashforth scheme coupled with an implicit Crank-Nicolson scheme $O(\Delta t^2)$
- Pressure treatment in the spectral space with the help of the modified wave number concept
- Parallel version (MPI implementation and pencil domain decomposition)

S. Laizet and E. Lamballais, JCP, 2009

S. Laizet *et al.*, CF, 2010

S. Laizet and N. Li, IJNMF, 2011

Computational domain and boundary conditions

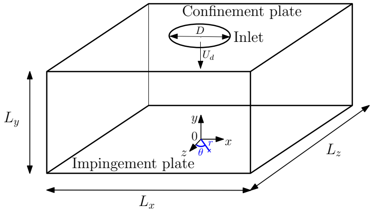

- Physical parameters : $Re = 10000$, $H/D = 2$, $Pr = 1$
- Numerical parameters :
  - $n_x = n_z = 1541 \Rightarrow \Delta x^+ \approx 10$
  - $n_y = 401 \Rightarrow 0.9 \lessapprox \Delta y^+ \lessapprox 40$
  - $\Delta t = 2.10^{-4}$

T. Dairay *et al.*, ETC14, 2013

Velocity

- Inflow : Mean velocity prescribed (power law) + synthetic pertubations
- Outflow : Buffer zone
- Top and bottom plates : No-slip condition

Temperature

- Inflow : Constant temperature T_j
- Outflow : Convective condition
- Top plate : Constant temperature T_j
- Bottom plate : Constant heat flux φ_p

Contents

Velocity statistics

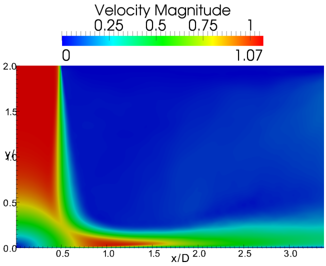

$|| \langle \mathbf{u} \rangle ||$

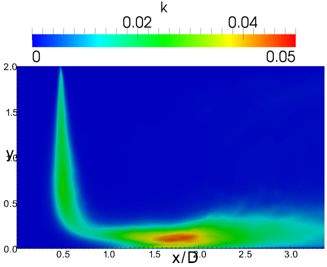

$\overline{u_i'^2}/2$

- Free jet region $(0.5 < y/D < 2)$: Potential core, low turbulence intensity on the jet axis ($u_y = U_{max}$), shear layer $r/D \approx 0.5$
- Stagnation region $(0 < y/D < 0.5$ and $r/D < 1.8)$: Axial to radial flow, boundary layer from the stagnation point, u_r increase, k maximum
- Wall jet region $(r/D > 1.8)$: radial velocity, u_r and k decrease

Temperature statistics

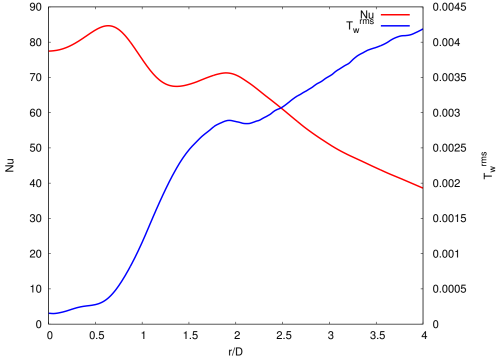

- Local minimum at the stagnation point : low turbulence level on the jet axis (potential core)
- Primary maximum at $r/D \approx 0.7$: structures issuing from the jet shear layer
- Secondary maximum at $r/D \approx 2$: linked with the region $1 \leq r/D \leq 2$ of high k

Contents

Flow animation : Q criterion colored by y/D

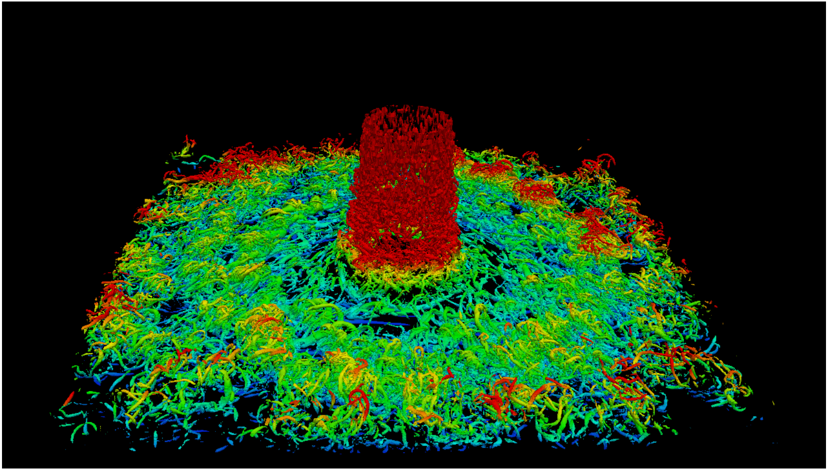

Large-scale organisation

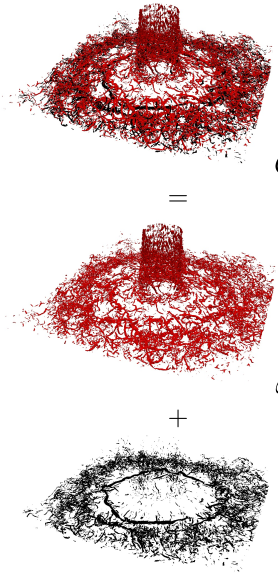

$Q = 70$

$=$

$\omega_\theta > 0$

$+$

$\omega_\theta < 0$

2D toroidal structures :

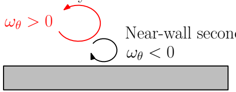

Heat transfer :

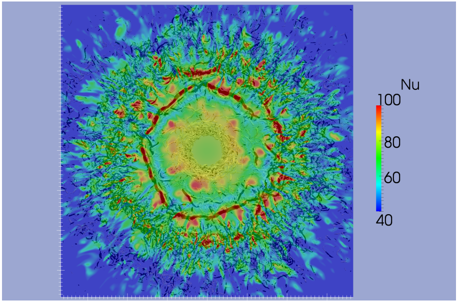

Small-scale organisation

Map $Nu \geq 80$

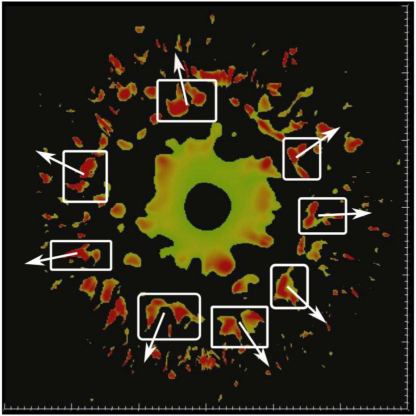

- Cold spots : extremely high heat transfer
- Radial stretching : filament propagation of cold spots

Hadziabdic et Hanjalic, JFM, 2008 ; Uddin *et al.*, IJHMT, 2013

Small-scale organisation

Isosurface $Q = 50$ and temperature map in the plane $r/D = 1.5$

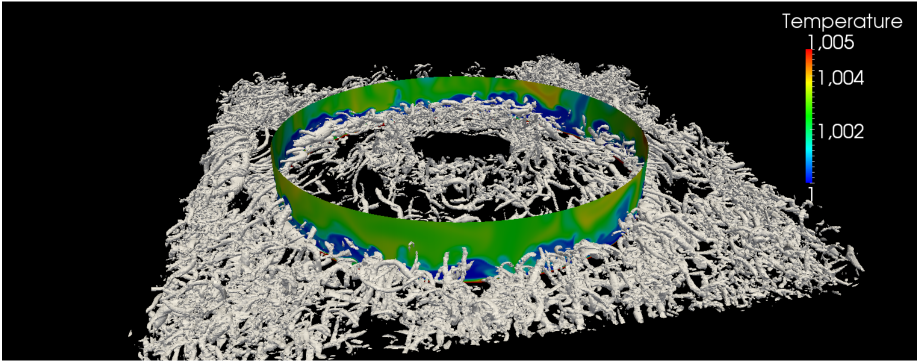

Small-scale organisation

Isosurface $Q = 50$ and temperature map in the plane $r/D = 1.5$

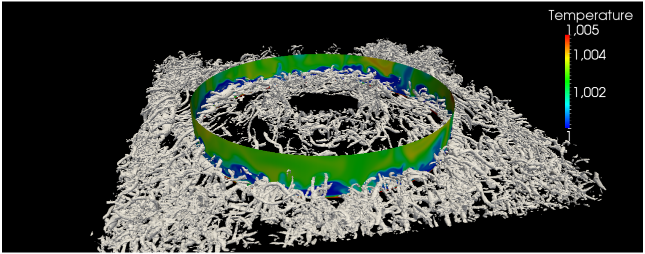

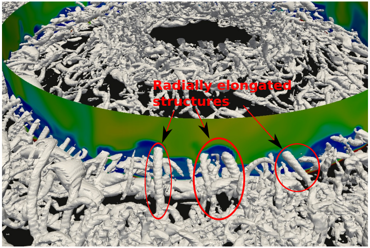

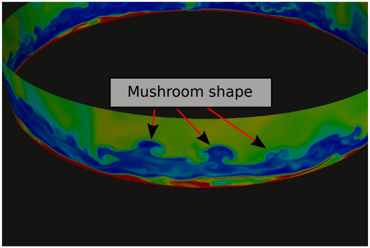

Instantaneous fields in the vicinity of a cold spot

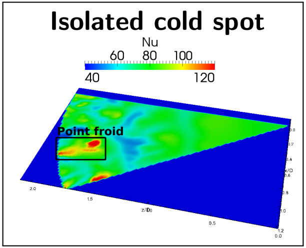

Instantaneous fields in the vicinity of a cold spot

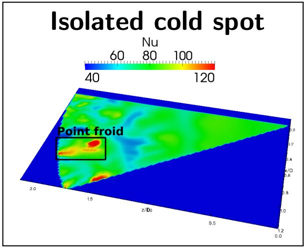

T in the plane $\theta = Cste$

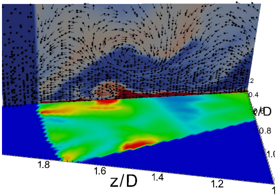

2D toroidal

Instantaneous fields in the vicinity of a cold spot

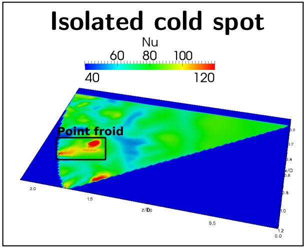

T in the plane $\theta = Cste$

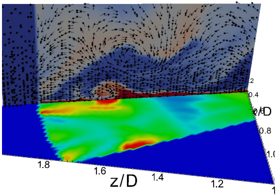

2D toroidal

Isosurface $Q = 10$

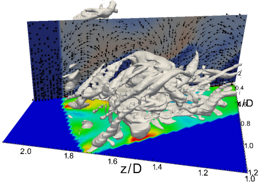

Instantaneous fields in the vicinity of a cold spot

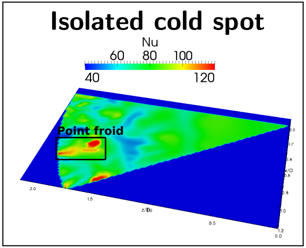

T in the plane $\theta = Cste$

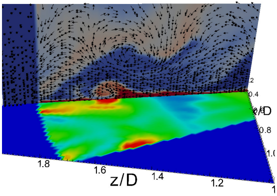

2D toroidal

Isosurface $Q = 10$

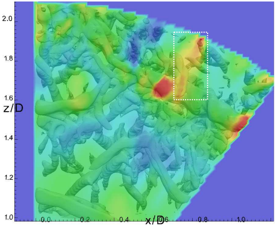

Radial structures

Instantaneous fields in the vicinity of a cold spot

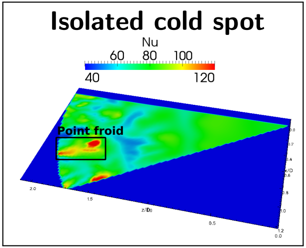

T in the plane $\theta = Cste$

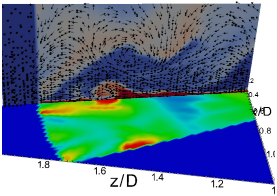

2D toroidal

Isosurface $Q = 10$

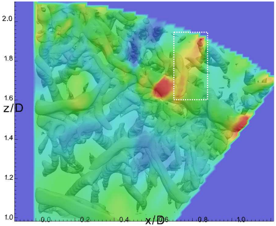

Radial structures

T in the plane $r/D = 1.77$

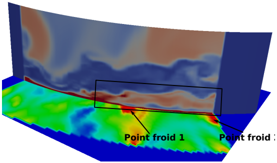

Azimuthal distortion

Spatio-temporal maps

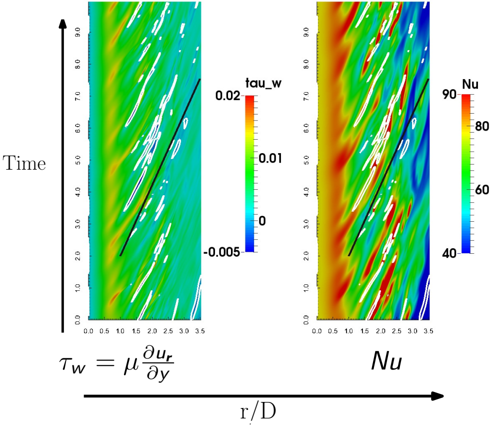

- For $r/D < 0.5$: steady evolution $\Longrightarrow$ local minimum of $\overline{Nu}$
- For $0.5 < r/D < 1$: periodical appearance of high heat transfer values $\Longrightarrow$ primary maximum of $\overline{Nu}$
- For $1 < r/D < 2.5$: secondary vortex and cold fronts convected at $U_c \approx 0.45 U_d \Longrightarrow$ increase of $\overline{Nu}$

Spatio-temporal maps

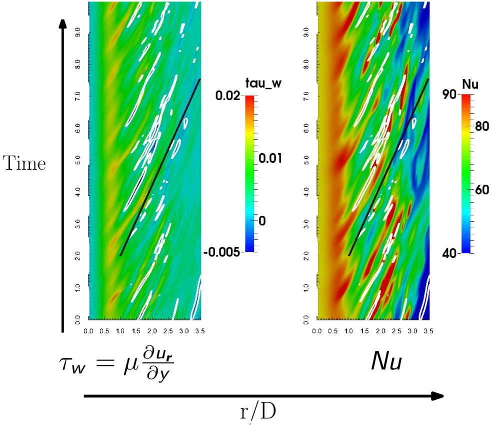

- For $r/D < 0.5$: steady evolution $\Longrightarrow$ local minimum of $\overline{Nu}$
- For $0.5 < r/D < 1$: periodical appearance of high heat transfer values $\Longrightarrow$ primary maximum of $\overline{Nu}$
- For $1 < r/D < 2.5$: secondary vortex and cold fronts convected at $U_c \approx 0.45 U_d$ $\Longrightarrow$ increase of $\overline{Nu}$

Spatio-temporal maps

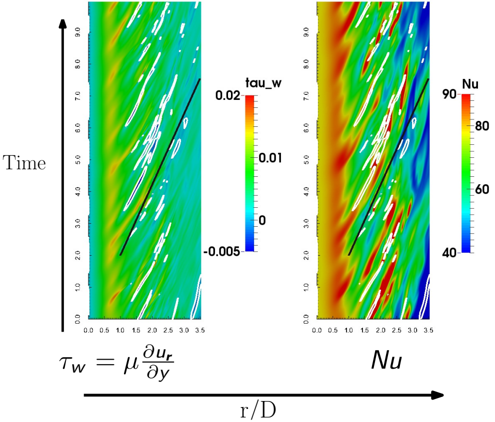

- For $r/D < 0.5$: steady evolution $\Longrightarrow$ local minimum of $\overline{Nu}$
- For $0.5 < r/D < 1$: periodical appearance of high heat transfer values $\Longrightarrow$ primary maximum of $\overline{Nu}$
- For $1 < r/D < 2.5$: secondary vortex and cold fronts convected at $U_c \approx 0.45 U_d$ $\Longrightarrow$ increase of $\overline{Nu}$

Probability Density Functions

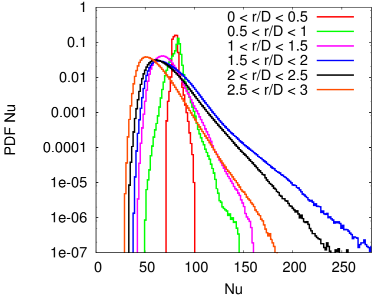

- For $1.5 \leq r/D \leq 2.5$ (blue and black curves) : highly skewed PDF with $Nu > 200 \Longrightarrow$ rare but extremely intense thermal events
- Most probable location of $\tau_w \leq 0$ in the range $1.5 \leq r/D \leq 2$
- Extreme events localised in the range $1.5 \leq r/D \leq 2.5$ with a maximum probability at $r/D \approx 2$

Probability Density Functions

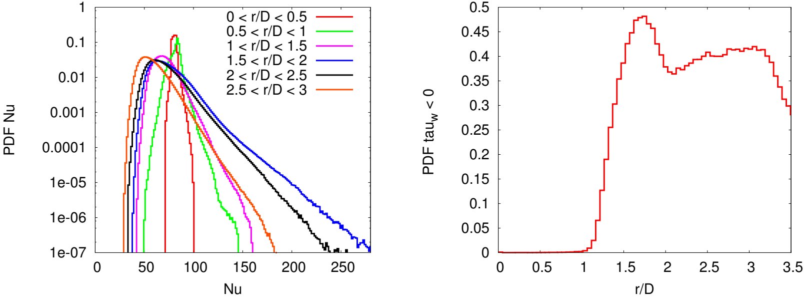

- For $1.5 \leq r/D \leq 2.5$ (blue and black curves) : highly skewed PDF with $Nu > 200 \Longrightarrow$ rare but extremely intense thermal events
- Most probable location of $\tau_w \leq 0$ in the range $1.5 \leq r/D \leq 2$
- Extreme events localised in the range $1.5 \leq r/D \leq 2.5$ with a maximum probability at $r/D \approx 2$

Probability Density Functions

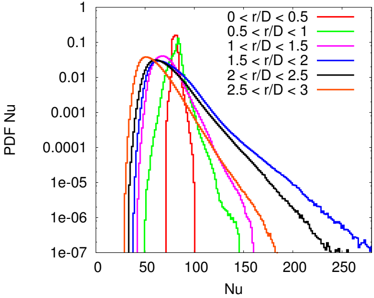

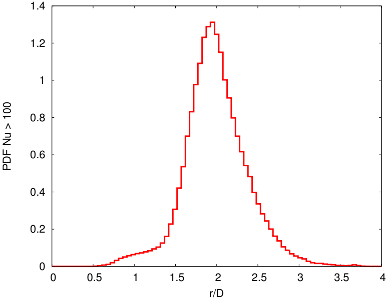

- For $1.5 \leq r/D \leq 2.5$ (blue and black curves) : highly skewed PDF with $Nu > 200 \Longrightarrow$ rare but extremely intense thermal events
- Most probable location of $\tau_w \leq 0$ in the range $1.5 \leq r/D \leq 2$
- Extreme events localised in the range $1.5 \leq r/D \leq 2.5$ with a maximum probability at $r/D \approx 2$

Cold spots detection and conditional averaging

Intermediate radial location $r/D = 1.75$

1. Selection of comparable instants
2. Detection of the azimuthal angles corresponding to a cold spot (threshold $S = 110$)
3. Conditional averaging operator $\langle f(r,\xi,y,t_0)\rangle_{Nu} = \frac{1}{N}\sum_{j=1}^{N} f(r,\theta_j+\xi,y,t_0)$
4. Temporal averaging of each conditionally averaged field

Temporal evolution of the azimuthally averaged

Nusselt number at $r/D = 1.75$

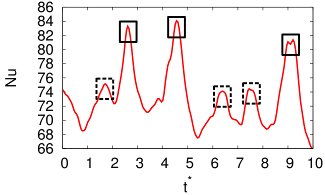

Cold spots detection and conditional averaging

Intermediate radial location $r/D = 1.75$

1. Selection of comparable instants
2. Detection of the azimuthal angles corresponding to a cold spot (threshold $S = 110$)
3. Conditional averaging operator $\langle f(r, \xi, y, t_0)\rangle_{Nu} = \frac{1}{N}\sum_{j=1}^{N} f(r, \theta_j + \xi, y, t_0)$
4. Temporal averaging of each conditionally averaged field

Temporal evolution of the azimuthally averaged

Nusselt number at $r/D = 1.75$

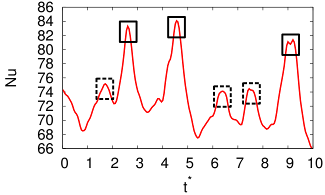

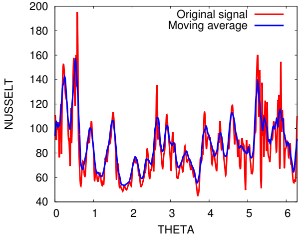

Cold spots detection and conditional averaging

Intermediate radial location $r/D = 1.75$

1. Selection of comparable instants
2. Detection of the azimuthal angles corresponding to a cold spot (threshold $S = 110$)
3. Conditional averaging operator $\langle f(r, \xi, y, t_0) \rangle_{Nu} = \frac{1}{N} \sum_{j=1}^{N} f(r, \theta_j + \xi, y, t_0)$
4. Temporal averaging of each conditionally averaged field

Temporal evolution of the azimuthally averaged

Nusselt number at $r/D = 1.75$

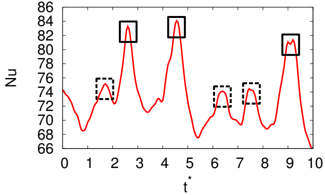

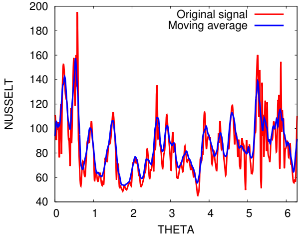

Cold spots detection and conditional averaging

Intermediate radial location $r/D = 1.75$

1. Selection of comparable instants
2. Detection of the azimuthal angles corresponding to a cold spot (threshold $S = 110$)
3. Conditional averaging operator $\langle f(r,\xi,y,t_0)\rangle_{Nu} = \frac{1}{N}\sum_{j=1}^{N} f(r,\theta_j+\xi,y,t_0)$
4. Temporal averaging of each conditionally averaged field

Temporal evolution of the azimuthally averaged

Nusselt number at $r/D = 1.75$

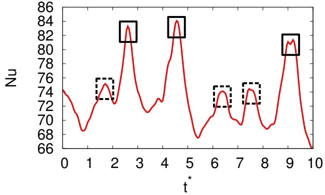

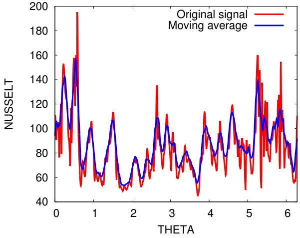

Aerothermal fields in the vicinity of a cold spot

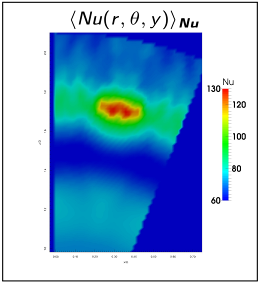

Aerothermal fields in the vicinity of a cold spot

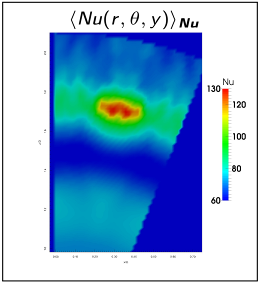

$\langle Nu(r, \theta, y)\rangle_{Nu}$ and $\langle T(r, \theta, y)\rangle_{Nu}$

in a plane $\theta = cste$

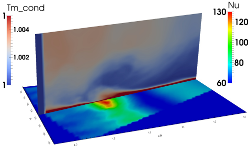

Cold fluid flux

Aerothermal fields in the vicinity of a cold spot

$\langle Nu(r,\theta,y)\rangle_{\boldsymbol{Nu}}$

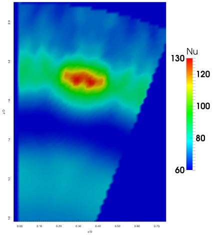

$\langle Nu(r,\theta,y)\rangle_{\boldsymbol{Nu}}$ and $\langle T(r,\theta,y)\rangle_{\boldsymbol{Nu}}$ in a plane $\theta = cste$

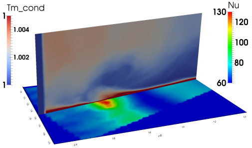

Cold fluid flux

Conditional mean streamlines

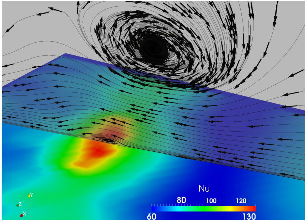

Primary and secondary vortices

Aerothermal fields in the vicinity of a cold spot

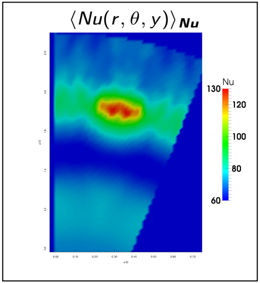

$\langle Nu(r,\theta,y)\rangle_{Nu}$ and $\langle T(r,\theta,y)\rangle_{Nu}$ in a plane $\theta = cste$

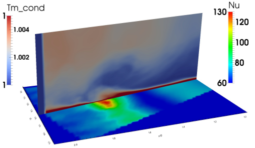

Cold fluid flux

Conditional mean streamlines

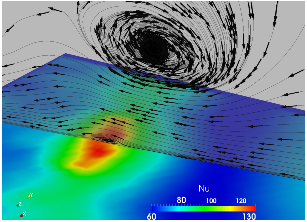

Primary and secondary vortices

Conditional mean streamlines projected in the near-wall plane $y/D = \Delta y_{min}$

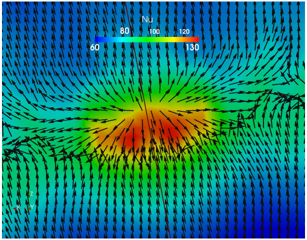

Contents

Unsteady processes and heat transfer distribution at the wall

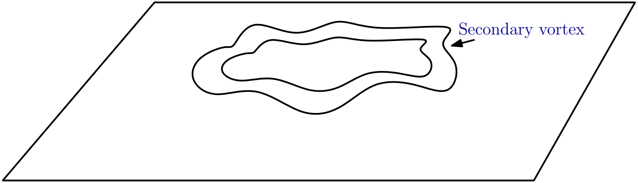

- Instantaneous visualisations
  - Large-scale toroidal organisation
  - Azimuthal distortion → cold spots
  - Radial stretching
- Spatio-temporal maps : cold fronts convected at the same velocity as the secondary vortex
- PDF : extremely high heat transfer linked with cold spots occurrence in the vicinity of the secondary maximum ($1.5 \leq r/D \leq 2.5$)
- Conditional averaging : cold fluid flux directed toward the impingement plate

Unsteady processes and heat transfer distribution at the wall

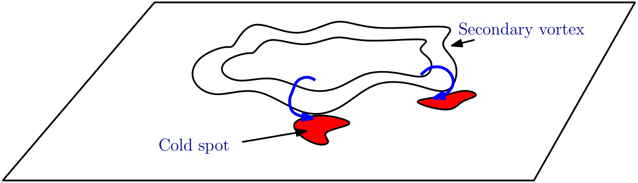

- Instantaneous visualisations
  - Large-scale toroidal organisation
  - Azimuthal distortion → cold spots
  - Radial stretching
- Spatio-temporal maps : cold fronts convected at the same velocity as the secondary vortex
- PDF : extremely high heat transfer linked with cold spots occurrence in the vicinity of the secondary maximum ($1.5 \leq r/D \leq 2.5$)
- Conditional averaging : cold fluid flux directed toward the impingement plate

Unsteady processes and heat transfer distribution at the wall

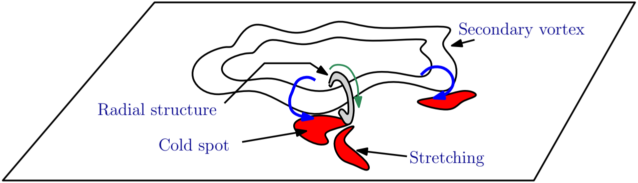

- Instantaneous visualisations
  - Large-scale toroidal organisation
  - Azimuthal distortion → cold spots
  - Radial stretching
- Spatio-temporal maps : cold fronts convected at the same velocity as the secondary vortex
- PDF : extremely high heat transfer linked with cold spots occurrence in the vicinity of the secondary maximum ($1.5 \leq r/D \leq 2.5$)
- Conditional averaging : cold fluid flux directed toward the impingement plate

Unsteady processes and heat transfer distribution at the wall

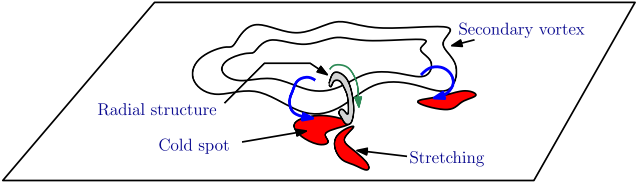

- Instantaneous visualisations
  - Large-scale toroidal organisation
  - Azimuthal distortion → cold spots
  - Radial stretching
- Spatio-temporal maps : cold fronts convected at the same velocity as the secondary vortex
- PDF : extremely high heat transfer linked with cold spots occurrence in the vicinity of the secondary maximum ($1.5 \leq r/D \leq 2.5$)
- Conditional averaging : cold fluid flux directed toward the impingement plate

Unsteady processes and heat transfer distribution at the wall

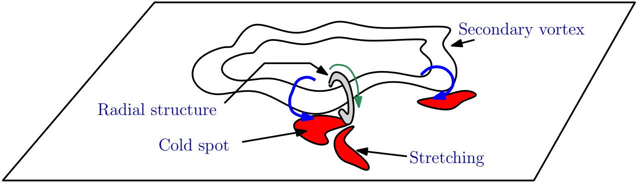

- Instantaneous visualisations
  - Large-scale toroidal organisation
  - Azimuthal distortion → cold spots
  - Radial stretching
- Spatio-temporal maps : cold fronts convected at the same velocity as the secondary vortex
- PDF : extremely high heat transfer linked with cold spots occurrence in the vicinity of the secondary maximum ($1.5 \leq r/D \leq 2.5$)
- Conditional averaging : cold fluid flux directed toward the impingement plate

Unsteady processes and heat transfer distribution at the wall

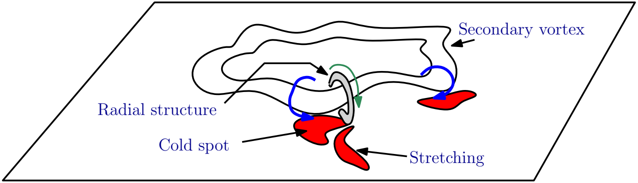

- Instantaneous visualisations
  - Large-scale toroidal organisation
  - Azimuthal distortion → cold spots
  - Radial stretching
- Spatio-temporal maps : cold fronts convected at the same velocity as the secondary vortex
- PDF : extremely high heat transfer linked with cold spots occurrence in the vicinity of the secondary maximum ($1.5 \leq r/D \leq 2.5$)
- Conditional averaging : cold fluid flux directed toward the impingement plate

Additional comment

The secondary maximum amplitude is reduced when using LES approaches → confirm the importance of the small-scale contribution to the mean heat transfer

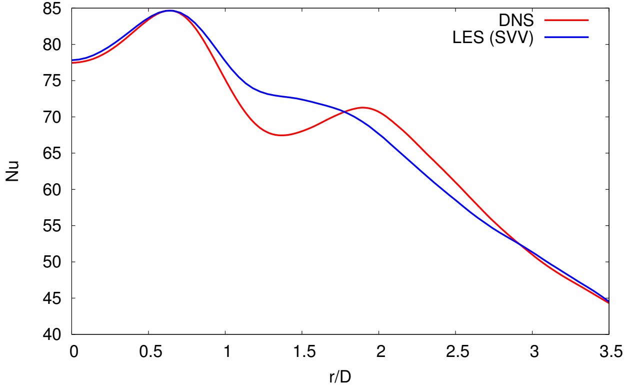

Thank you